General Disclaimer

One or more of the Following Statements may affect this Document

- This document has been reproduced from the best copy furnished by the organizational source. It is being released in the interest of making available as much information as possible.

- This document may contain data, which exceeds the sheet parameters. It was furnished in this condition by the organizational source and is the best copy available.

- This document may contain tone-on-tone or color graphs, charts and/or pictures, which have been reproduced in black and white.

- This document is paginated as submitted by the original source.

- Portions of this document are not fully legible due to the historical nature of some of the material. However, it is the best reproduction available from the original submission.

NASA TECHNICAL MEMORANDUM

NASA TM X-73555

NASA TM X-73555

(NASA-TM-X-73555) CHARACTERISTICS OF AN ANECHOIC CHAMBER FOR FAN NOISE TESTING (NASA) 32 p HC A03/MF A01 CSCL 14B

N77-18168

Unclas
G3/09 13951

CHARACTERISTICS OF AN ANECHOIC CHAMBER FOR FAN NOISE TESTING

by Joseph A. Wazyniak, Loretta M. Shaw, and
Jefferson D. Essary
Lewis Research Center
Cleveland, Ohio 44135

TECHNICAL PAPER to be presented at the
International Gas Turbine Conference sponsored by the
American Society of Mechanical Engineers
Philadelphia, Pennsylvania, March 25-30, 1977

CHARACTERISTICS OF AN ANECHOIC CHAMBER FOR FAN NOISE TESTING

Joseph A. Wazyniak, Loretta M. Shaw, and Jefferson D. Essary

A B S T R A C T

Acoustical and mechanical design features of NASA Lewis Research Center's engine fan noise facility are described. Acoustic evaluation of the 1,420-m^3 (50,000-ft^3) chamber, which is lined with an array of stepped wedges, is described. Results from the evaluation in terms of cut-off frequency and non-anechoic areas near the walls are detailed.

Fan models with 0.51-m (20-in.) diameters are electrically driven to 20,600 RPM in either the inlet mode (drawing air from the chamber) or exhaust mode (discharging air into the chamber) to facilitate study of both fore and aft fan noise. Inlet noise characteristics of the first fan tested, the JT8D Refan, are discussed and compared to full-scale levels. Turbulence properties of the inlet flow and acoustic results are compared with and without a turbulence reducing screen over the fan inlet.

CHARACTERISTICS OF AN ANECHOIC CHAMBER FOR FAN NOISE TESTING

Joseph A. Wazyniak, Loretta M. Shaw, and Jefferson D. Essary

INTRODUCTION

Since 1967 NASA Lewis has been investigating turbofan aircraft engine noise and methods to reduce it. Because a dominant source of noise in a turbofan engine is the fan, special emphasis has been placed on the study of that engine component. A major element in the research effort has been the acoustic testing of full-scale (1.83-m (6-ft.) diameter) prototype fans in an outdoor facility (ref. 1). This series of fans, covering the pressure ratio range from 1.2 to 1.6, has been acoustically evaluated and some of the results correlated in reference 2.

During the course of this testing it became apparent that the outdoor facility had certain drawbacks. 1) Testing time was severely limited due to inclement weather conditions, 2) fabrication and assembly time for various configurations was quite lengthy, 3) hardware and operational costs for full-scale fans were rather high, and 4) the arrangement of the facility drive-shaft and its supports contributed to inlet flow distortions which produced source noise uncharacteristic of the clean inflow existing in flight (ref. 3). The possibility of overcoming these problems by testing scale-model fans in an anechoic chamber lead to the design and construction of the facility described herein.

The initial step in the process of bringing the facility to its fully operational status was a detailed acoustic evaluation of the chamber, designed to determine the frequency and spatial ranges over which free field propagation is maintained. The next step was the actual testing of a 0.407 scale-model fan, for which extensive acoustic data from an engine incorporating the full-scale fan were available (refs. 4 and 5). The final step

was to investigate the inlet flow characteristics with and without a turbulence reducing screen over the inlet.

This paper summarizes the facility design features, the acoustic evaluation results, the results of the initial fan tests, including the validity of acoustic scaling, and the turbulence characteristics of the fan inflow.

CHAMBER REQUIREMENTS

The main objective in the design of the chamber was to provide an indoor anechoic facility that enables far field acoustic measurements to be made on both 0.51-m (20-in.) diameter research fans and scale-model jet exhaust configurations 5-cm (2-in.) to 15-cm (6-in.) in diameter. In meeting this objective, the design required a minimization of inlet flow distortions to the fan that could possibly cause turbulence induced fan noise. Thus, no physical obstructions were to be placed in the vicinity of the fan inlet, and a uniform flow distribution into the fan was to be provided by having the chamber surfaces aspirate in the region surrounding the inlet.

It was anticipated that fans to be tested in the chamber would have a range of tip speeds from 215-m/sec (700-ft/sec) to 550-m/sec (1800-ft/sec), a range of pressure ratios from 1.1 to 2.5, and a maximum flow rate of 35 kg/sec (80-lb/sec). These parameters determined the design of both the air handling system and the fan drive system. The design low cut-off frequency of 150 Hz was determined by the needs of the jet noise rig. The cut-off frequency is defined here as the point where the percent energy absorption drops to less than 99%, i.e., a sound reduction of 20 dB for a single reflection.

FACILITY LAYOUT

The location of the five rooms which comprise the noise facility are shown in the plan view of figure 1. The sound isolation room allows air to pass into or out of the facility, while keeping outdoor noise in the chamber at a minimum. The fan drive room houses the electric motor, gearbox, air handling system for the fan, and fan instrumentation. The jet room contains the muffler and piping for the jet rig, and thrust stand, and various jet instrumentation. The facility control room houses the facility controls, data acquisition systems, and data reduction systems.

The anechoic chamber, which encompasses a volume of 1,420-m^3 (50,000-$ft.^3$) and contains 1,110-m^2 (12,000-$ft.^2$) of surface area, is 5.2-m (17-ft.) high, 15.9-m (52-ft.) wide, and 13.4-m (44-ft.) long. The protrusion in the chamber opposite the jet rig allows an extra distance for diffusion before the jet blast impacts the chamber wall.

A. Flow Systems

In measuring the inlet noise of the fan, air is drawn from the chamber into the fan. The paths in which the air enters and leaves the facility are best seen by following the arrows in the facility elevation view (figure 2). Ambient air enters the facility through the intake on the left. It then divides and enters the chamber through the silencer and through the wall, floor, and ceiling aspirating areas. In this mode the bulk of the air passes through the silencer, and thus this mode is referred to as non-aspirating.

In the aspirating mode, however, the silencer is blocked and all the air is forced to enter the chamber through the aspirating areas. The air which passes over the ceiling wedges enters the chamber between the ceiling wedges near the fan and also circulates behind the wall wedges and enters

the chamber along the wall areas shown in figure 1. The aspirating floor area is supplied with air through a slot under the silencer. The air then passes under the floor wedges and aspirates into the chamber only in the area of the fan rig. Aspiration is attained by spacing the acoustic wedges approximately 2.5-cm (1-in.) apart, and letting the air enter between them. All of the data reported herein was obtained with the chamber in the aspirating mode.

The air which passes through the fan is exhausted vertically from the facility through the ducting in the drive room (figure 2). Throttling valves located in these ducts allow for adjustment of the fan back pressure, while the mufflers prevent valve noise from propagating into the chamber or out of the facility.

Aft fan noise measurements are obtained by turning the fan around and exhausting into the chamber. In this mode air is drawn into the facility through the ducting in the drive room, is exhausted out of the chamber through the silencer opposite the fan, and leaves the facility through the intake/exhaust above the sound isolation room.

B. Fan Drive System

The fan drive system is located in the facility as shown in figure 1. The wall which separates the drive room from the chamber was designed to have a high transmission loss to prevent motor and gear noise from being transmitted to the chamber. Similarly, mounting the drive system on a separate foundation isolates any vibrations generated in the drive system from the chamber.

The drive motor is a variable speed induction motor capable of producing 5.2×10^6 watts (7000 horsepower). A step-up gearbox connected to the motor provides rotational capabilities to 20,600 RPM. The entire drive system is capable of rotation in either direction to allow a fan to be driven

from either the inlet (for aft noise) or the aft end (for inlet noise).

C. Acoustic Design

The frequency range of interest for the scale fans to be tested in the chamber is from 200 Hz to 40 kHz. During fan testing, microphones are placed on a 90° arc with a 6.1-m (20-ft.) radius from the fan inlet to ensure far field measurements. To achieve free field sound levels over these frequency and distance ranges, the chamber was lined with 76-cm (30-in.) deep fiberflass wedges. An isometric view of a wedge is shown in figure 3. Impedance tube measurements have shown that the low frequency cut-off point of this type of "stepped" wedge is 150 Hz.

The wedges were constructed by cutting 5-cm (2-in.) thick sheets of fiberglass to the various depths shown in figure 3, enclosing these pieces with a fiberglass cloth for protection in handling, and then putting the base of the wedge into a wire cage for structural support. The wall and ceiling wedges were then hung with a 10-cm (4-in.) space between the base of the wedge and the wall to allow for a resonating air space behind the wedge. The floor wedges sit on top of an expanded metal grating that lies 20-cm (8-in.) above the chamber concrete floor. The photograph of the chamber in figure 4 shows the wedge arrangement. The wedges on the ceiling are oriented such that the tips of the wedges run parallel with one another across the length of the ceiling, while the tips of the wall wedges are parallel and form vertical lines from the floor to the ceiling. The floor wedges are arranged in a pattern whereby four 1.2-m (4-ft.) long wedges are placed side by side and each group is oriented on the floor such that their tips are perpendicular to those of the surrounding groups.

ACOUSTIC EVALUATION

In order to confirm that free field conditions were achieved in the chamber, a detailed acoustic evaluation was carried out. Measurements of the sound pressure level (SPL) fall-off as a function of distance from a noise source were made over a range of frequencies from 100 Hz to 40 kHz. Comparison of the SPL fall-off in the chamber with that of free space, 6 dB per doubling of distance, indicates the frequency range over which the chamber can be considered anechoic.

In the evaluation, the noise source was placed at a point corresponding to the fan inlet plane location. Four .64-cm (.25-in.) microphones were traversed radially outward from the source to points 10.7-m (35-ft.) from the source. These four traverses were at azimuth angles of 0°, 30°, 60°, and 90° with respect to the fan centerline. The traversing systems consisted of a thin cable stretched directly under the ceiling wedges upon which a small cart and microphone support system rolled. The 30°, 60°, and 90° traversing systems can be seen in the photograph of the chamber (figure 4).

In order to adequately investigate the frequency range of interest, 100 Hz to 40 kHz, three noise sources were employed in the evaluation. Both a pure tone source and two broadband sources were used. The pure tone source offered a severe test of the chamber because such a source generates only one wavelength and thus any chamber resonances are easily detected in the form of standing waves. On the other hand, even though the many wavelengths present in a broadband source tend to average out any resonances at particular frequencies, the broadband sources are more typical of the type of sound that will be measured in the chamber.

A 30-cm (1-ft.) diameter speaker powered by a function generator and amplifier was used to produce pure tones from 100 Hz to 5 kHz. At higher frequencies the speaker output level was too low to give an acceptable signal to noise

ratio with the microphone 10.7-m (35-ft.) from the speaker. Thus, a 1.6-cm (5/8-in.) open-ended jet, tuned for peak power at 30 kHz, was used to study the high frequency characteristics of the room. The third source used was the 0.5-m (20-in.) diameter model fan. With the fan running at constant speed, the microphones were traversed in 30-cm (1-ft.) increments from 3.0-m (10-ft.) to 10.7-m (35-ft.) from the fan. During the traverses involving the speaker, the pure tone level was measured through a wave analyzer set to a bandwidth of 50 Hz, while in the traverses involving the jet and fan, 1/3-octave data were measured. The data from the fan tests were obtained by taking the average of three samples, each sample being a 4-second integrated value. These data were then fitted to the inverse square curve, i.e., a 6 dB SPL drop per doubling of distance, by a least squares method in order to obtain a measure of the deviations from the inverse square law. In order to investigate only the fan broadband noise, 1/3-octave bands containing fan tones were ignored.

In the original chamber configuration the floor wedges were placed directly on the concrete floor and the expanded metal grating was placed above the wedges to facilitate movement within the chamber (fig. 5(a)). The presence of this grating, however, led to severe standing wave patterns at frequencies near 5 kHz. Figure 5(b) shows the analog traces obtained in the evaluation using a pure tone for both the original configuration with the grating above the wedges and the present configuration with the wedges on top of the grating. The drastic reduction in the standing wave pattern obtained when the grating was placed under the wedges necessitated this to be the standard chamber configuration. In this configuration movement inside the chamber is accomplished by locally removing the floor wedges. Although movement within the chamber is now more time consuming and somewhat irritating in

moving the fiberglass wedges, the acoustic benefits far outweigh these inconveniences.

Figure 6 presents the results of the traversing tests for the 60° microphone over the entire frequency range. Shown in the figure are the analog traces of the SPL fall-off as a function of distance from the source when using either the speaker or jet as the source, along with the discrete points obtained when using the fan as the source. All data above 1 kHz have been corrected for the effect of atmospheric absorption according to the methods outlined in reference 6. The inverse square law curve is also shown on each plot for ease in evaluation of the curves. Inspection of the figure shows a large standing wave at the 100 Hz tone. At higher frequencies, smaller standing waves tend to form at distances greater than 6.0-m (20-ft.) from the source. The pure tone at 5 kHz produced standing wave patterns more predominant than those generated by other frequencies near 5 kHz. It is assumed that this phenomena is related to the wedge geometry.

The deviations from the inverse square law near the standard microphone distance, 6.1-m from the source, are of prime importance. The maximum deviations as a function of frequency in the distance range from 4.6-m (15-ft.) to 7.6-m (25-ft.) are shown in figure 7 for the various sources. Figure 7(a) presents the results of the pure tone and jet tests while figure 7(b) contains the results of the fan tests.

Inspection of figure 7(a) shows that large deviations were observed over much of the frequency range for the 90° microphone. Traverses along this angle placed the microphone as close as 23-cm (9-in.) to the wedges on the drive room wall. Stationary microphone data were taken at the 80° angle to ensure that the effects felt at 90° were not still present. This data fell in line with the other angles and thus only the 90° microphone is close enough to the wedges to be considered to be in a non-anechoic region.

For the pure tone source, the deviations are relatively constant from 200 Hz to 5kHz. An increase in the deviations at 100 Hz is apparent at 0^{o} and 30^{o} and, as shown in figure 6, a large deviation appeared at 8.5-m (28-ft.) for the 60^{o} microphone. Because of this marked increase at 100 Hz and the relatively constant deviations obtained at frequencies at and above 200 Hz, the chamber low frequency cut-off point is considered to be 200 Hz. The 1/3-octave deviations obtained from the broadband fan source are shown in figure 7(b). As would be expected, the deviations obtained in this test are lower than those obtained when using the pure tone source. Most of these deviations are less than 1.0 dB, and in general are about half of those obtained at the same frequencies when using a pure tone source.

An acoustic evaluation of the chamber was also performed for the portion of the chamber containing the jet exhaust facility. The measurements showed that the anechoic characteristics of the chamber in this location were similar to those described above. In addition, it was noted that because large amounts of dry air are exhausted into the chamber during a jet test, significant gradients in the temperature and humidity developed in the chamber. Thus, in order to accurately calculate the atmospheric absorption of sound at high frequencies, it is necessary to make localized temperature and humidity measurements and then compute the atmospheric absorption for each microphone individually.

Having established the anechoic characteristics of the chamber, the next step was to quantize the background noise features of the facility. Because high sound levels are generated by a fan, no special sound absorbing material was built into the chamber to attenuate outside noise. The facility is located in an area surrounded by other test rigs and is situated above heavy machinery used to run these various rigs. The concrete floor and concrete block walls of the facility do not transmit most of the higher frequencies,

but relatively high levels are present in the chamber at the lower frequencies. Figure 8 shows a normal background spectrum obtained in the chamber, the spectrum obtained with only the motor and gearbox systems running, and a typical spectrum obtained with the fan running at a low speed. Although the low-frequency background level is relatively high, at frequencies above 200 Hz these levels are well below those obtained during fan testing.

FAN TEST RESULTS

The final step in determining the chamber's usefulness as a tool in fan noise research was to compare acoustic data obtained from a scale version of a fan to that obtained in the full-scale version of the same design. The first fan tested in the facility was a 0.407-scale model of the JT8D Refan stage for which extensive full-scale engine static acoustic data were available (ref. 4).

In the Refan program a single-stage fan was designed to replace the two-stage fan currently being used in the JT8D engine. To obtain the detailed aerodynamic performance of the new design, a 0.407-scale model of the split flow fan stage was built and tested in the NASA Lewis single-stage compressor facility (ref.7). Following completion of the aerodynamic testing, the fan was acoustically tested in the anechoic chamber.

A cross-sectional view of the JT8D Refan stage installed in the fan noise facility as well as a list of some of the design parameters are given in figure 9. The large lipped, contoured inlet is a 0.407-scale model of the one used during the static full-scale engine tests, and models the flight inlet contour downstream of the throat.

Static pressure taps in the inlet throat plane were used to compute the fan weight flow, while two rakes downstream of the exit guide vanes were used in computing the bypass weight flow, pressure ratio, and efficiency. These few aerodynamic measurements along with fan speed were sufficient to

accurately reproduce the operating points obtained in the compressor facility and in the engine tests.

In this installation, both the core and bypass flow discharged into a common air collector before entering the discharge ducts (fig. 9). Thus, the core and bypass regions operated at the same pressure ratio, and it was not possible to vary the bypass ratio in order to obtain those ratios observed on the engine. Over the range of speeds studied, however, the bypass ratios obtained on the fan did not differ from the engine by more than 10 percent except at low speed points.

A fan operating line for the scale fan was obtained by scaling the fan operating points obtained during the static engine acoustic tests. In taking acoustic data, the scale fan was set at corrected speeds corresponding to those of the engine during acoustic testing, and then loaded by closing the discharge valves to obtain the desired operating point. Nine .64-cm (.25-in.) microphones on a 6-m (20-ft.) radius from the inlet and spanning azimuth angles from 0° to 80° were employed in obtaining the acoustic data. Three 4-second integrated values of SPL for 1/3-octave bands from 200 Hz to 40 kHz were obtained at each operating condition. The average SPL values were then corrected for atmospheric absorption according to the methods detailed in reference 8.

To scale this data to a full-size fan, corrections were then made for the effects of the weight flow ratio and rotative speed ratio between the two fans. This was accomplished by adding 7.8 dB, i.e. 10 log (scale factor)^2, to each SPL, and shifting each of these new SPL values down four 1/3-octave bands, i.e. 10 log (scale factor). These data were then extrapolated to a 61-m (200-ft.) sideline for comparison with static engine data, some of which is reported in reference 4.

In making a comparison between fan and engine perceived noise levels (PNL's), the engine data must be chosen so that engine points used in the comparison have PNL's that are controlled by the fan inlet source noise and not another engine noise source. In addition the engine source noise should not be altered by the presence of any acoustic treatment. Thus, engine data used in this paper was obtained with the engine in a completely hardwall configuration. Comparisons of scaled fan spectra with those of the engine show that in the inlet hemisphere the fan source noise controls the engine PNL's except at speeds greater than 90% of design. At these higher speeds jet noise becomes increasingly important, and at angles greater than 60° both jet noise and aft fan noise influence the PNL's.

A comparison of the PNL's from the scaled fan and full-scale engine at 60° is shown in figure 10 where the PNL's are plotted as a function of fan speed. The scaled fan data follows the trend of the engine data in that the PNL rises steadily with speed in the subsonic tip speed region, increases sharply as the fan tip speed becomes supersonic, and then slowly falls off as design speed is approached. The sharp increase in PNL as the relative tip speed becomes supersonic is due to the formation of multiple pure tones (MPT's).

In addition to following the changes in full-scale engine PNL's with speed, the scaled fan data also closely match the engine's PNL directivity patterns (figure 11). At a low speed setting (50% of design) the excellent agreement between the engine and scaled fan PNL's is apparent. At 70% design speed (approach power) the agreement is excellent near the fan axis but the scaled levels are 2 to 3 PNdB higher at the angles of peak fan noise. Jet noise raises the engine PNL's above those of the scaled fan at design speed (takeoff power), especially at angles greater than 60°, where both jet and aft fan noise significantly contribute to the PNL.

The differences in PNL's between the engine and scaled fan are best explained by comparing 1/3-octave spectra at the 60° angular position. At design speed the engine and scaled fan spectra agree closely at frequencies above 1kHz (figure 12(a)). However, differences in the MPT structure between 500 Hz and 1.25 kHz along with the presence of engine jet noise centered at 200 Hz account for the higher PNL's observed on the engine. The uniqueness of each fan fabrication and installation can account for the variation in the MPT structure. Figure 12(b), which shows the dominance of the blade passage tone and its harmonic at approach power, indicates somewhat higher broadband and blade passage tone levels were obtained by scaling the fan data. The scaled fan broadband levels were found to be slightly higher than those of the engine at all angles for subsonic tip speed points; while the tone levels, which control the PNL's, were found to exceed those of the engine primarily at angles greater than 30°. This problem of obtaining similar blade passage tone levels in different static facilities is further addressed in the next section, but it should be noted at this point that the scaling procedures used here cannot be fully tested until methods are developed to control fan inflow disturbances and turbulence which may affect fan source noise during static testing. However, the good agreement in directivity patterns and speed related effects between the full scale fan in the engine and the scaled fan in the anechoic chamber establishes the chamber as a viable tool for fan noise research.

INLET TURBULENCE STUDY

In the past few years several investigations (refs. 9, 10, 11) have found differences between fan stage noise data obtained in static and in-flight tests. As shown in figure 13, the most obvious difference in-flight is the nearly complete absence of the random fluctuations of the blade

passage tone with time. These data, which were measured in the inlets of both the engine and scale fan, clearly show that the static cases have similar time histories for the tone sound pressure levels. These fluctuations are evidence that some unsteady disturbances exist in the inlet flow. It has been postulated that these disturbances in outdoor test stands result from convected atmospheric turbulence and ground vortices (refs. 12 and 13). In the chamber these disturbances may arise from the way in which the air enters the chamber or from problems associated with the fan's close proximity to the wall behind the inlet.

In an initial experiment to investigate the inlet flow characteristics in the chamber, hot film measurements of inlet turbulence intensity and scale were made with and without a conical screen around the inlet. The screen shown in figure 14, was constructed of 0.25-mm (0.01-in.) diameter fiberglass strands formed in a 15 X 17 mesh pattern with an open area ratio of 72 percent. The average values of the hot film measurements made in the inlet showed a significantly lower axial intensity when the screen was over the inlet (fig. 15(a)). The axial length scale of the turbulence was also found to decrease, especially at points near the inlet wall (fig. 15(b)).

Along with the changes detected in the inlet turbulence characteristics with the screen over the inlet a change was also noted in the noise generated by the fan. Although the blade passage tone of the JT8D Refan stage is cut-on, and thus should propagate to the far field by the theory of Tyler and Sofrin (ref. 13), a reduction in the level of the tone was observed at some points with the screen over the inlet (figure 16). The fact that no change in the broadband noise occurred when the screen was placed over the inlet and because no change was noted in the blade passage tone levels at 50% and 76% speed with the screen in place indicate that

the screen had no apparent transmission loss associated with it.

Because the fluctuations of the tone level were still present (fig. 13), it appears that the noise facility still does not completely model conditions found in flight. Further tests with inlet turbulence modifiers on a cut-off fan should yield more meaningful results because of the increased sensitivity of the tone to inlet disturbances and the virtual disappearance of cut-off tones when exposed to an environment simulating flight (ref. 15).

SUMMARY OF RESULTS

The NASA Lewis fan noise facility enables testing of both inlet and aft fan noise on 0.51-m (20-in.) diameter research fans in an indoor anechoic environment. The facility has been designed to accommodate fans with pressure ratios to 2.5 and weight flows up to 35-kg/sec (80-lb/sec). Results of the evaluation to determine the facility's usefulness as a tool in fan noise research were as follows.

1. Sound intensities in the anechoic chamber follow the inverse square law within 2.0 dB for pure tones from 200 Hz to 5kHz, and within 1.0 dB for 1/3-octave data of a broadband source from 200 Hz to 40 kHz. The entire chamber is anechoic except for areas within approximately 0.6-m (2-ft.) of the acoustical wedges, which for a typical fan installation, allows data to be taken over a range of azimuth angles from 0° to 80°. Background noise levels in the chamber are well below those generated by a fan.

2. Comparison of acoustic data from a 0.407-scale model fan and an engine incorporating the full-scale fan shows that the scaled fan data has similar directivity patterns and follows the same trends as the full-scale data when fan speed is altered. A complete evaluation of the scaling procedures is not possible at this time because both model and full scale blade passage tone levels are subject to the uncertainties associated with static testing.

3. Inlet axial turbulence intensities are approximately 4 percent in the free-stream with axial length scales ranging from 0.6-m (2-ft.) in the free-stream to 2.0-m (6.5-ft.) near the outer wall. A turbulence reducing screen over the inlet reduced the intensities by nearly a factor of two and reduced the length scales near the outer wall approximately 0.3-m (1.0-ft.). The screen also reduced the average blade passage tone level, but the unsteadiness of the level with time, a characteristic not present in flight data, indicates that further investigations into turbulence reducing devices is warranted.

REFERENCES

1. Leonard, Bruce R.; Schmiedlin, Ralph F.; Stakolich, Edward G.; and Newmann, Harvey E.: Acoustic and Aerodynamic Performance of 6-Foot-Diameter Fans for Turbofan Engines. Part 1 - Design of Facility and QF-1 Fan. NASA TN D-5877, 1970.

2. Heidmann, M. F.; and Feiler, C. E.: Noise Comparisons from Full-Scale Fan Tests at NASA Lewis Research Center. AIAA Paper 73-1017, Oct. 1973.

3. Povinelli, Frederick P.; Dittmar, James H.; and Woodward, Richard P.: Effects of Installation Caused Flow Distortion on Noise From a Fan Designed for Turbofan Engines. NASA TN D-7076, 1972.

4. Burdsall, E. A.; Brochu, F. P.; Scaramella, V. M.: Results of Acoustic Testing of the JT8D-109 Refan Engines. PWA-5298, NASA CR-134875, 1975.

5. Douglas Aircraft Company: DC-9 Flight Demonstration Program with Refanned JT8D Engines. MDC J4518, NASA CR-134860, 1975.

6. Bass, H. E.; Shields, F. D.: Atmospheric Absorption of High Frequency Noise and Application to Fractional-octave Bands. NASA CR-2760, 1976.

7. Moore, Royce D.; Kovich, George; Tysl, Edward R.: Aerodynamic Performance of 0.4066-Scale Model of JT8D Refan Stage. NASA TM X-3356, 1975.

8. Montegani, Francis J.: Some Propulsion System Noise Data Handling Conventions and Computer Programs Used at the Lewis Research Center. NASA TM X-3013, 1974.

9. Cumpsty, N. A.; and Lowrie, B. W.: The Cause of Tone Generation by Aero-Engine Fans at High Subsonic Tip Speeds and the Effect of Forward Speed, ASME Paper 73-WA/GT-4, 1973.

10. Merriman, J. E.; and Good, R. C.: Effect of Forward Motion on Fan Noise, AIAA Paper 75-464, 1975.

11. Roundhill, J. P.; and Schaut, L. A.: Model and Full Scale Test Results Relating to Fan Noise In-Flight Effects, AIAA Paper 75-465, 1975.

12. Hanson, D. B.: A Study of Subsonic Fan Noise Sources. AIAA Paper 75-466, March 1975.

13. Hodder, Brent K.: An Investigation of Possible Causes for the Reduction of Fan Noise in Flight. AIAA 3rd Aero-Acoustics Conference, AIAA Paper 76-585, Palo Alto, CA. July 1976.

14. Tyler, J. M.; and Sofrin, T. G.: Axial Flow Compressor Noise Studies. SAE Trans., vol. 70, 1962, pp. 309-332.

15. Heidmann, M. F.; and Dietrich, D. A.: Simulation of Flight-Type Engine Fan Noise in the NASA Lewis 9 X 15 Anechoic Wind Tunnel. NASA TM X-73540, 1976.

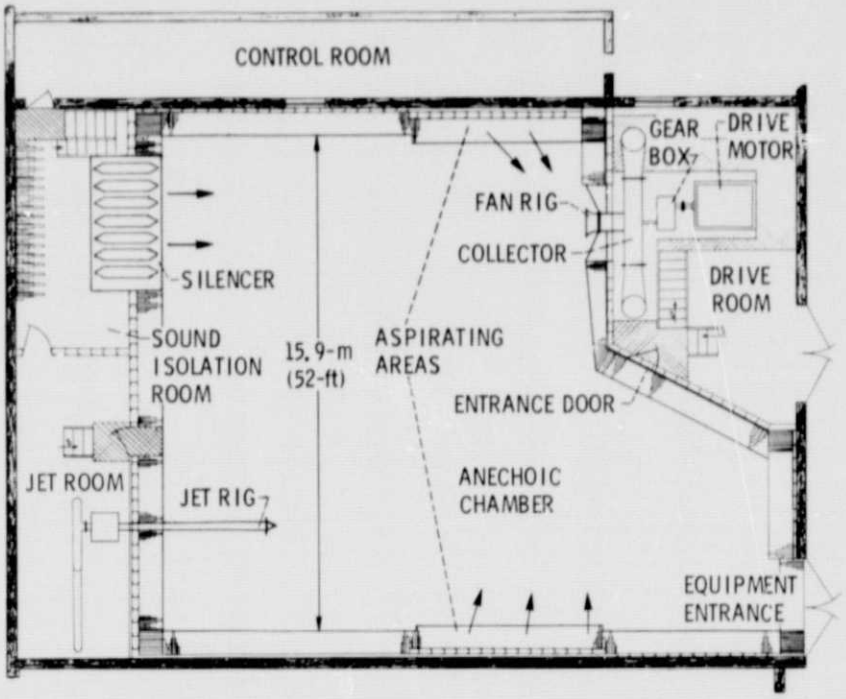

Figure 1. - Noise facility floor plan.

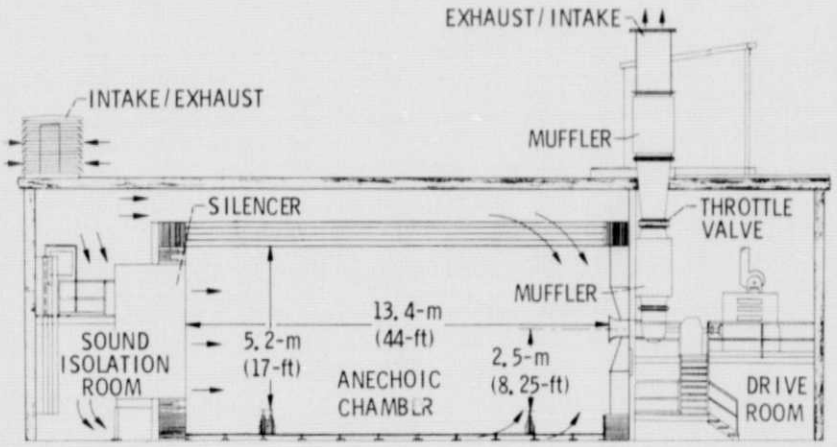

Figure 2. - Noise facility elevation view.

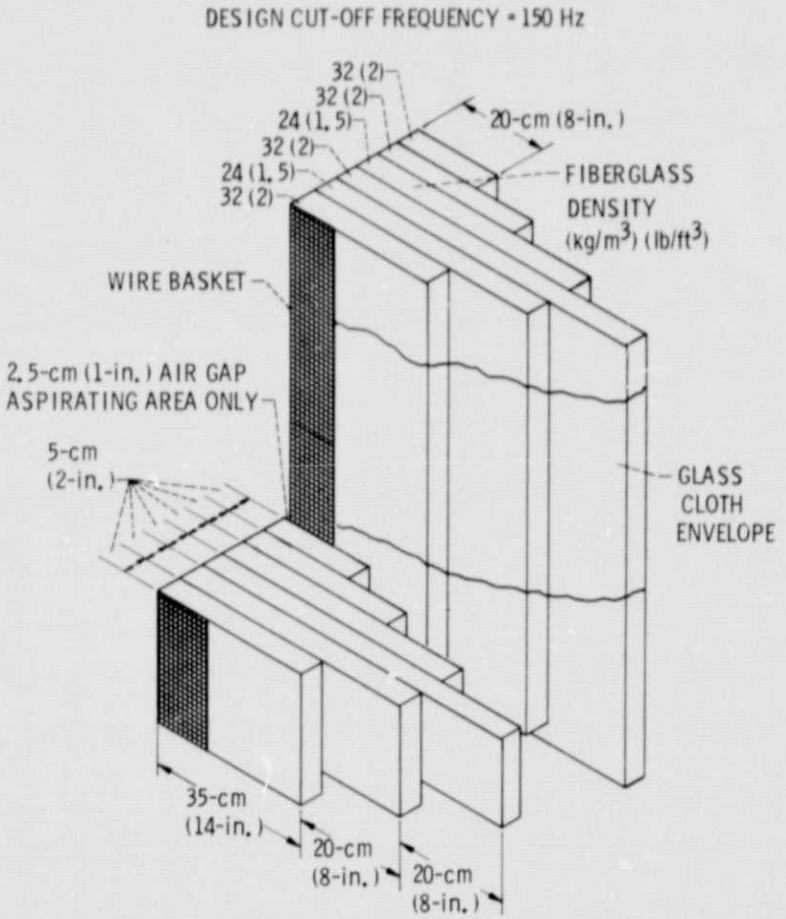

Figure 3. - Isometric view of typical acoustical wedge used in the Anechoic chamber.

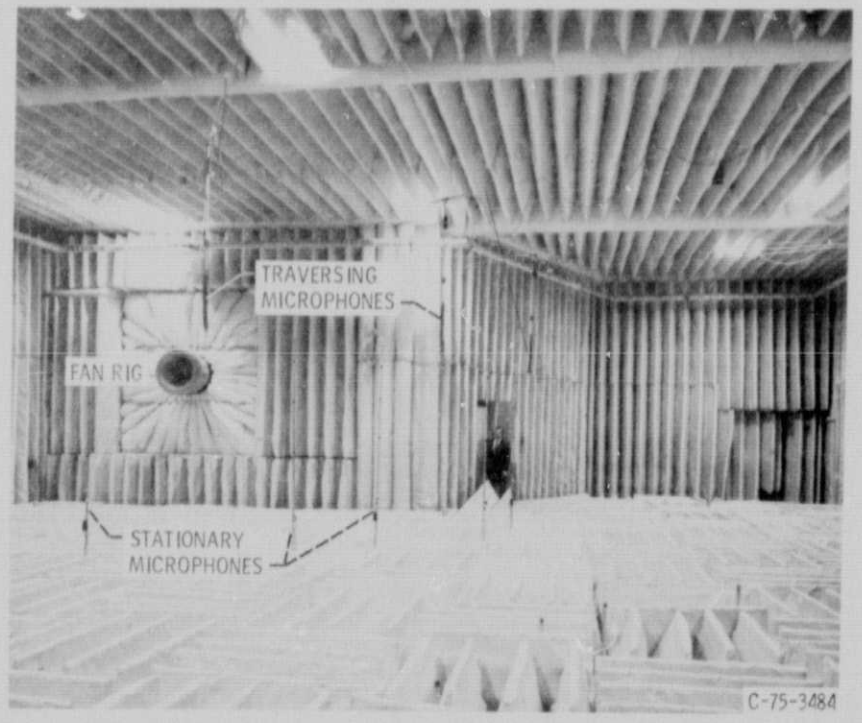

Figure 4. - Facility view showing fan test area.

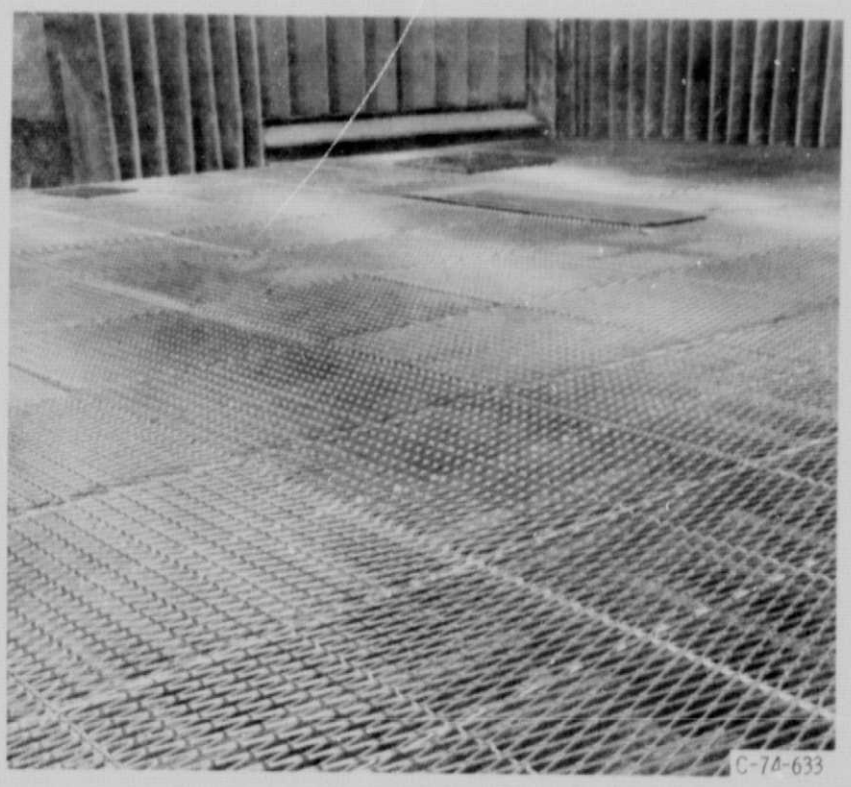

(a) Floor grating as originally installed in anechoic chamber.

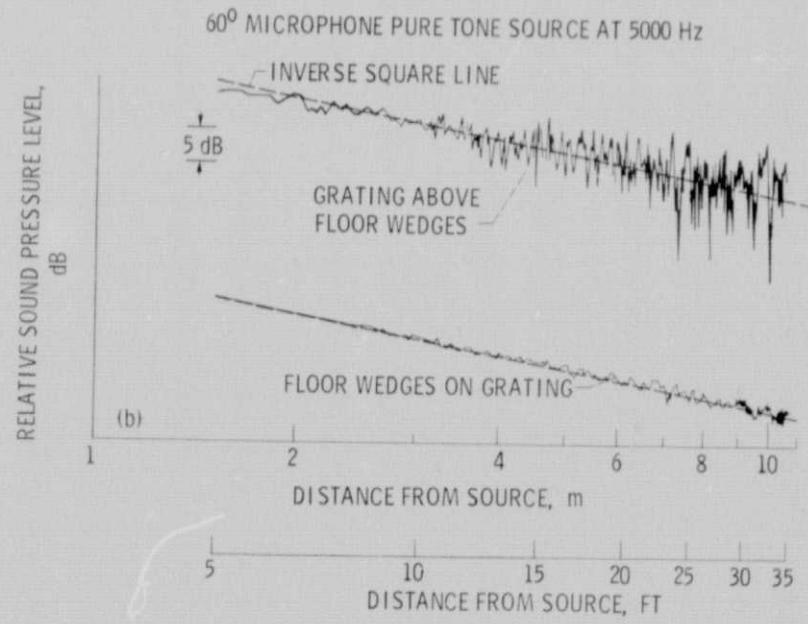

Figure 5. - Chamber evaluation data obtained with the expanded metal grating over the floor wedges and with the floor wedges on top of the grating.

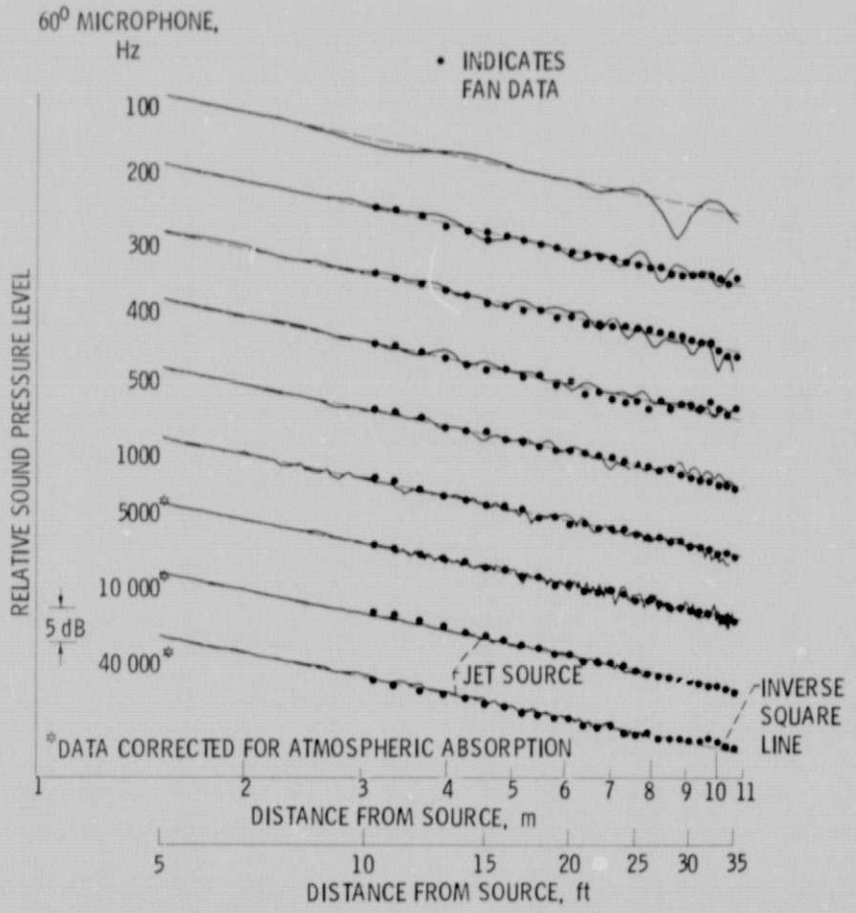

Figure 6. - Inverse square calibration data showing analog traces obtained with a pure tone source and jet source, as well as discrete data from fan source.

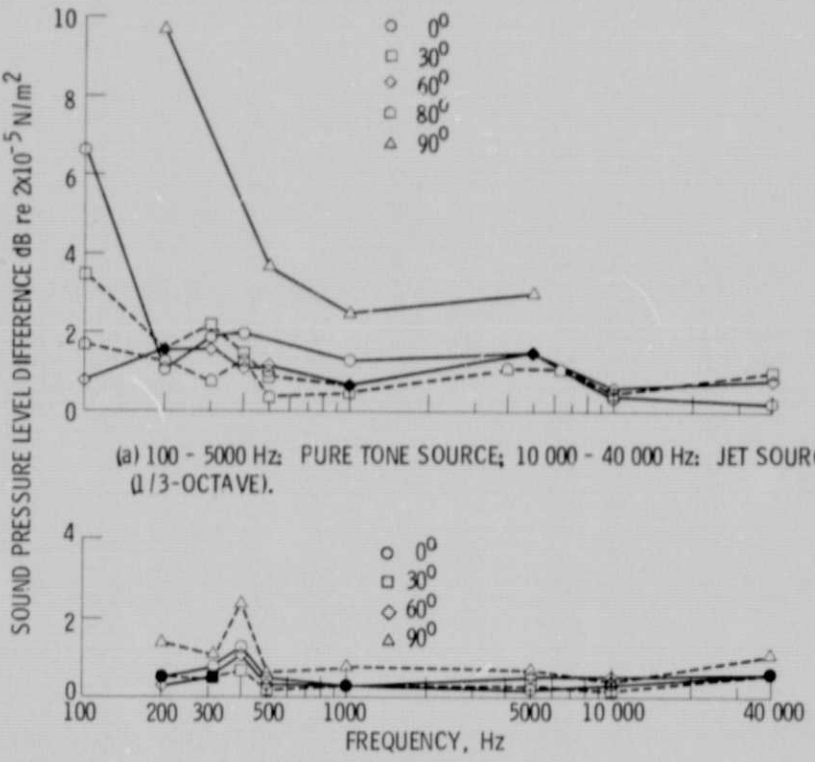

(a) 100 - 5000 Hz: PURE TONE SOURCE; 10 000 - 40 000 Hz: JET SOURCE (1/3-OCTAVE).

(b) 200 - 40 000 Hz: FAN BROADBAND SOURCE (1/3-OCTAVE).

Figure 7. - Maximum deviations from inverse square law over 4.6-m (15') to 7.6-m (25') range as a function of frequency.

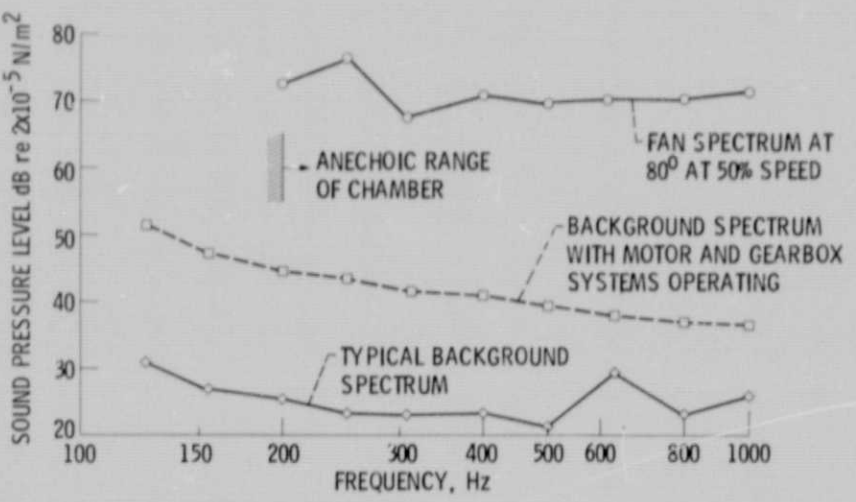

Figure 8. - Comparison of chamber background noise levels and typical fan noise levels.

DESIGN PARAMETERS

WEIGHT FLOW PER UNIT ANNULUS AREA	185.48 kg/sec-m^2 (42.0 lb/sec-ft^2)
WEIGHT FLOW	35.01 kg/sec (77.2 lb/sec)
BYPASS RATIO	2.032
BYPASS STAGE TOTAL PRESSURE RATIO	1.672
CORE STAGE TOTAL PRESSURE RATIO	1.642
BYPASS STAGE ADIABATIC EFFICIENCY	0.815
CORE STAGE ADIABATIC EFFICIENCY	0.855
ROTATIVE SPEED	18323 rpm
TIP SPEED	487.5 m/sec (1600 ft/sec)

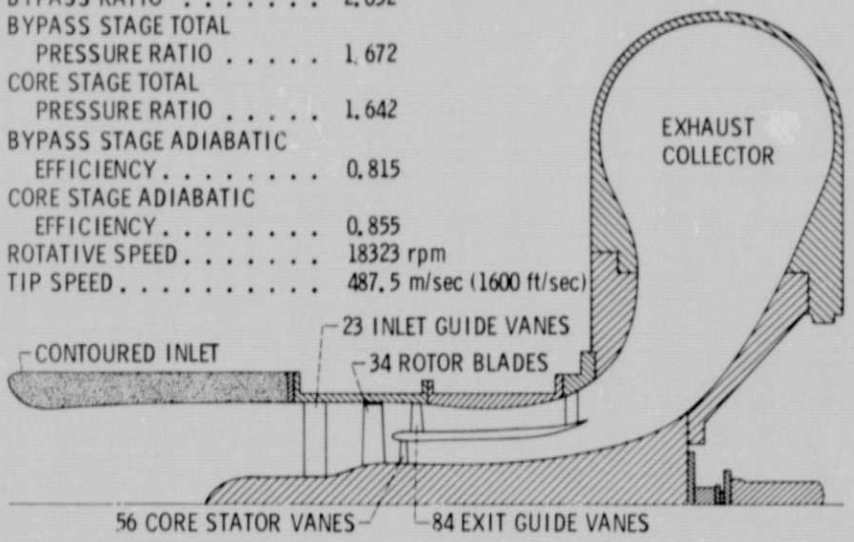

Figure 9. - Cross-sectional view of JT8D refan stage in fan noise facility and table of design parameters.

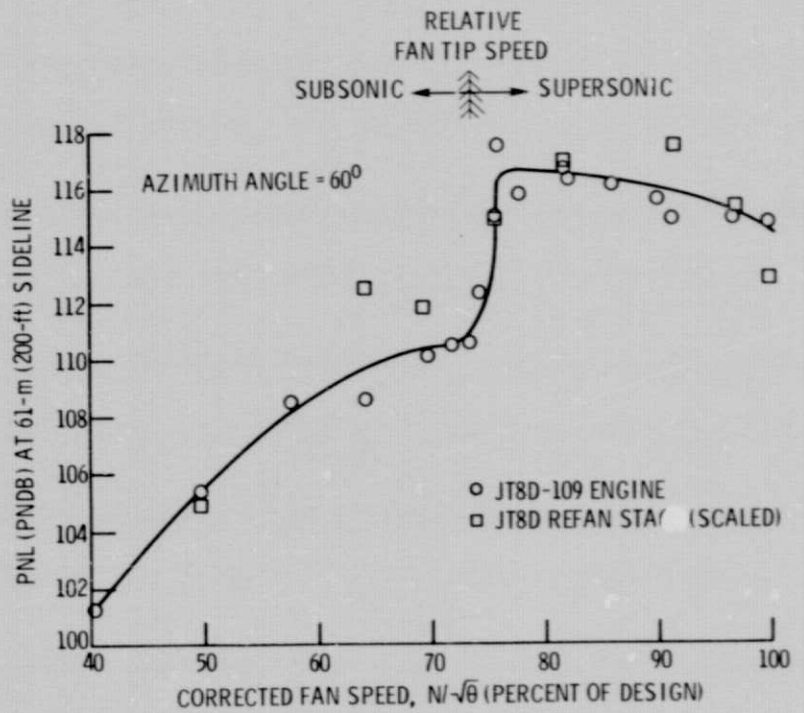

Figure 10. - PNL variation with speed at azimuth angle of 60° for JT8D refan engine and scaled fan.

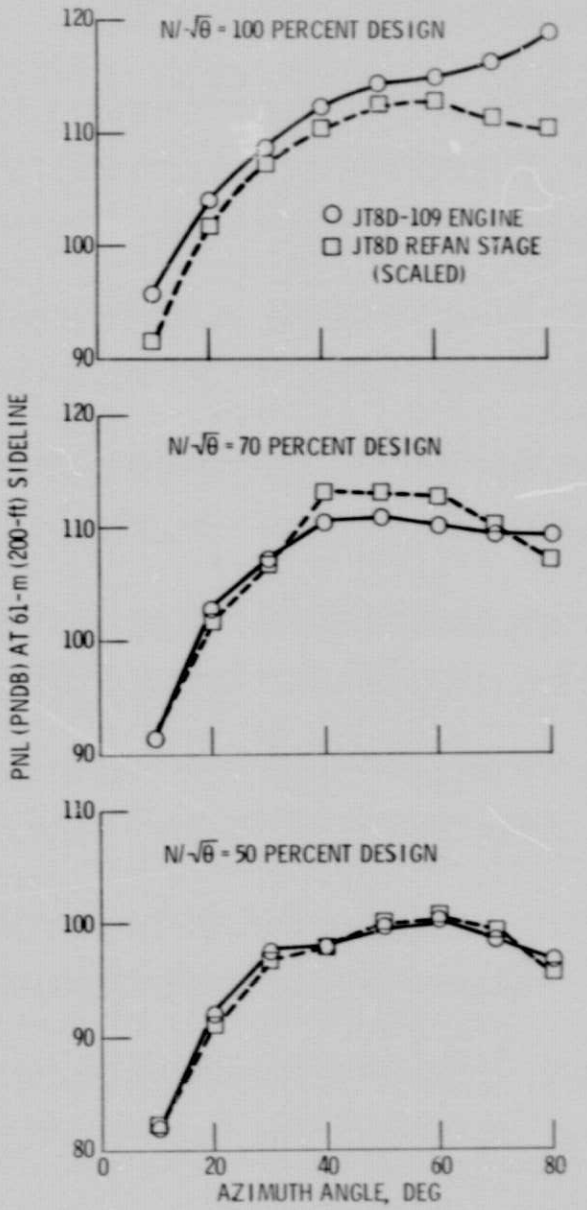

Figure 11. - PNL variation with angle for JT8D refan engine and scaled fan.

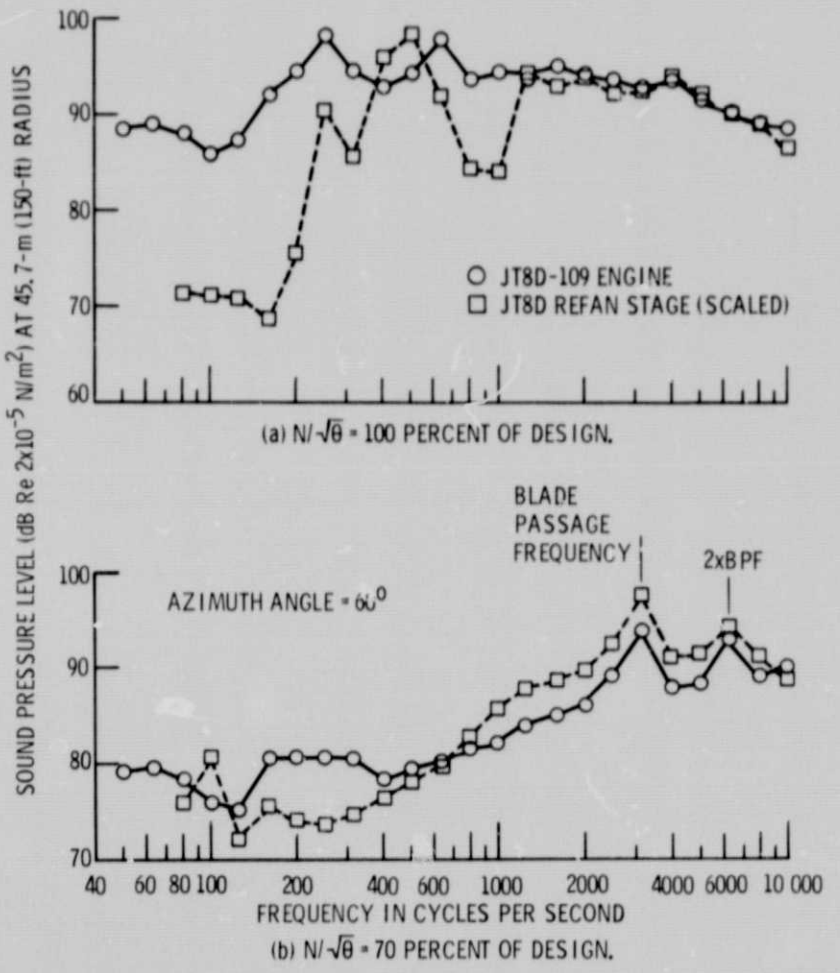

Figure 12. - Comparison of 1/3-octave SPL's at 45.7-m (150-ft) radius as a function of frequency for JT8D refan engine and scaled fan.

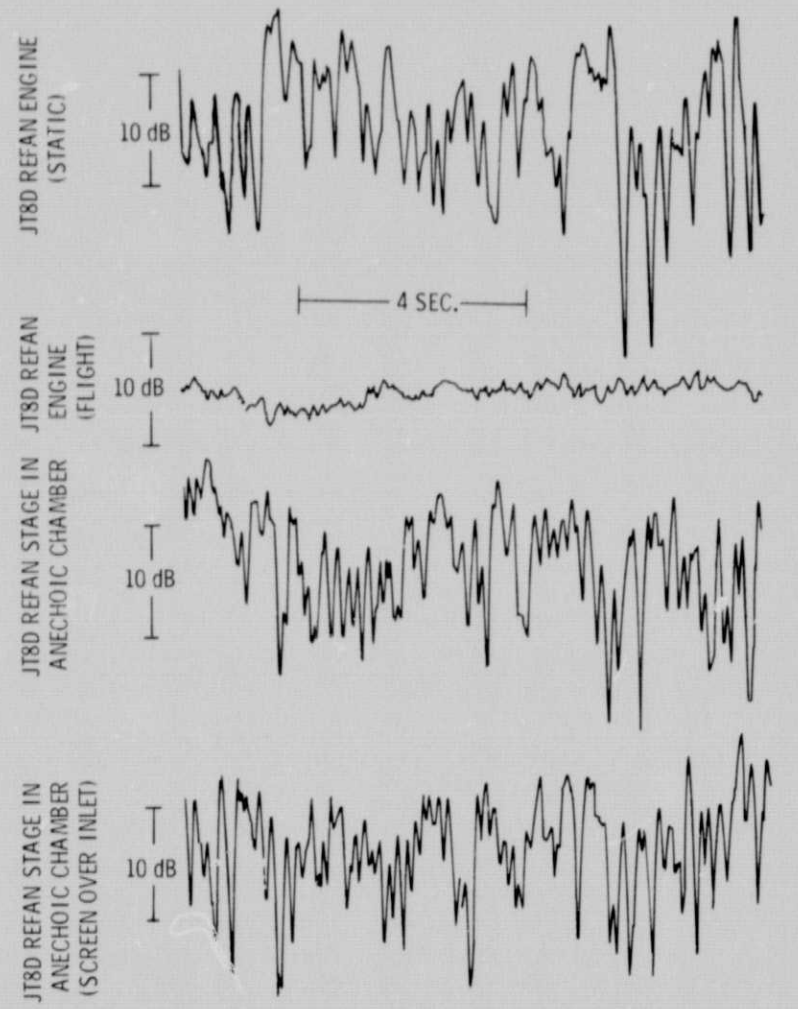

Figure 13. - Time variation in blade passage frequency tone levels in inlet ducts of JT8D refan engine on DC-9 aircraft and in anechoic chamber. $N/\sqrt{\theta}$ = 50 percent of design.

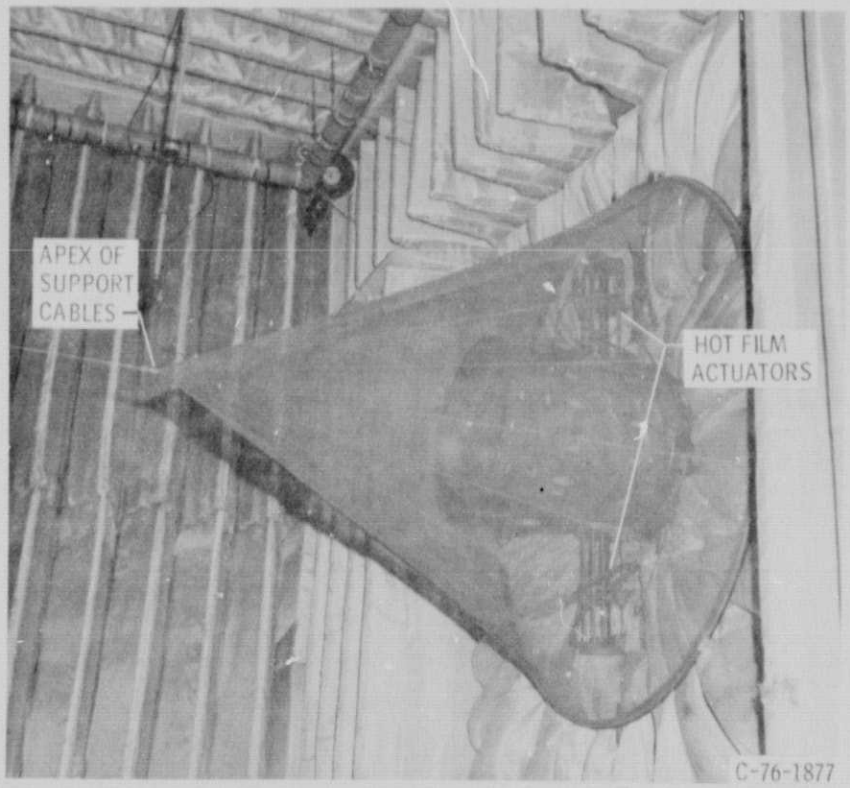

Figure 14. - Conical screen mounted over fan inlet.

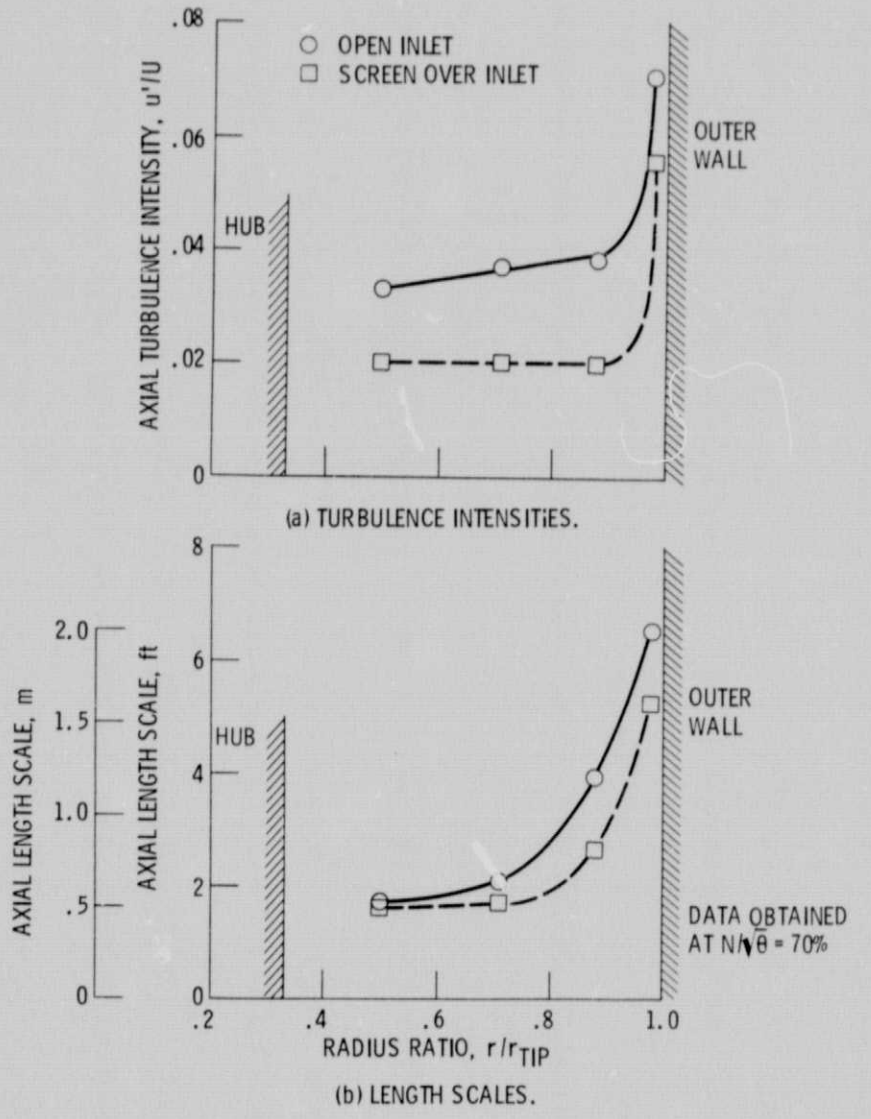

Figure 15. - Comparison of inlet hot film results with and without conical screen in place.

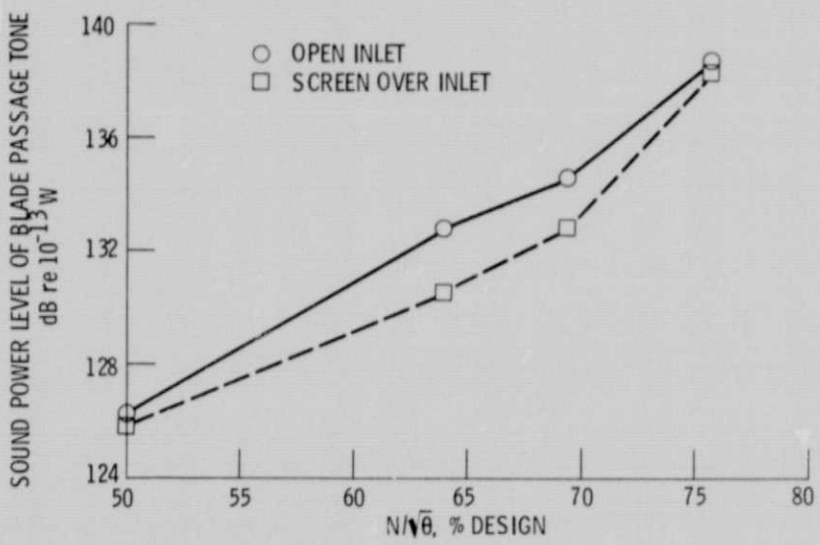

Figure 16. - Comparison of blade passage tone level with and without conical screen in place.